Naunyn-Schmiedeberg's Archives of Pharmacology (2024) 397:5131–5144
https://doi.org/10.1007/s00210-023-02935-2

RESEARCH

Synergistic induction of apoptosis in lung cancer cells through co-delivery of PLGA phytol/α-bisabolol nanoparticles

Chandramohan Kiruthiga[1] · Devasahayam Jaya Balan[1] · Nagaiah Hari Prasath[1] · Muthushanmugam Manikandakrishnan[2] · Sakthivel Jafni[1] · Narayanasamy Marimuthu Prabhu[2] · Shunmugiah Karutha Pandian[1] · Kasi Pandima Devi[1]

Received: 2 August 2023 / Accepted: 27 December 2023 / Published online: 19 January 2024

Abstract

This study explored the potential of poly-(lactic-co-glycolic) acid (PLGA) nanoparticles to enhance the effectiveness of anticancer treatments through combination therapy with phytol and α-bisabolol. The encapsulation efficiency of the nanoparticles was investigated, highlighting the role of ionic interactions between the drugs and the polymer. Characterization of PLGA-Phy+Bis nanoparticles was carried out using DLS with zeta potential and HR-TEM for size determination. Spectrophotometric measurements evaluated the encapsulation efficiency, loading efficiency, and in vitro drug release. FTIR analysis assessed the chemical interactions between PLGA and the drug actives, ensuring nanoparticle stability. GC-MS was employed to analyze the chemical composition of drug-loaded PLGA nanocarriers. Cytotoxicity was evaluated via the MTT assay, while Annexin V-FITC/PI staining and western blot analysis confirmed apoptotic cell death. Additionally, toxicity tests were performed on L-132 cells and in vivo zebrafish embryos. The study demonstrates high encapsulation efficiency of PLGA-Phy+Bis nanoparticles, which exhibit monodispersity and sizes of 189.3±5nm (DLS) and 268±54 nm (HR-TEM). Spectrophotometric analysis confirmed efficient drug encapsulation and release control. FTIR analysis revealed nanoparticle structural stability without chemical interactions. MTT assay results demonstrated the promising anticancer potential of all the three nanoparticle types (PLGA-Phy, PLGA-Bis, and PLGA-Phy+Bis) against lung cancer cells. Apoptosis was confirmed through Annexin V-FITC/PI staining and western blot analysis, which also revealed changes in Bax and Bcl-2 protein expression. Furthermore, the nanoparticles exhibited non-toxicity in L-132 cells and zebrafish embryo toxicity tests. PLGA-Phy+Bis nanoparticles exhibited efficient encapsulation, controlled release, and low toxicity. Apoptosis induction in A549 cells and non-toxicity in healthy cells highlight their clinical potential.

Keywords Lung cancer · Apoptosis · PLGA · Nanoparticles · Phytol · α-Bisabolol · Co-delivery

Introduction

Lung cancer is a deadly disease that affects millions of people worldwide. There are various therapies available for treating lung cancer, including chemotherapy, radiation therapy, targeted therapy, and immunotherapy. However, each of these therapies has its limitations and has been shown to develop resistance, which can reduce their effectiveness over time (Harrison et al. 2022). In addition, the increased efficacy of the chemo drug combination leads to a rise in adverse effects and off-target toxicity. Therefore, there has been a lot of interest in creating new natural-based chemotherapy regimens for non-small-cell lung cancer (NSCLC). Furthermore, urrent studies are exploring the use of nanoformulations, which involve the encapsulation of drugs within nanoparticles (NPs) (Norouzi and Hardy 2021; Gavas et al. 2021). This approach can improve drug delivery to the tumor site, reduce systemic toxicity, and enhance drug efficacy. As a viable alternative, administration of NPs with chemotherapeutic combinations has demonstrated an integrative manner to both improving reactions and minimizing adverse effects. NPs can lessen

✉ Kasi Pandima Devi
devikasi@yahoo.com; pdevik@alagappauniversity.ac.in

[1] Department of Biotechnology, Alagappa University, Karaikudi 630 003, Tamil Nadu, India

[2] Disease Control and Prevention lab, Department of Animal Health and Management, Alagappa University, Karaikudi 630 003, Tamil Nadu, India

exposure to off-target sites by accumulating drugs inside tumors preferentially(Gavas et al. 2021). Furthermore, carefully designed, dual-drug-loaded NPs can be used to deliver chemotherapies in a synergistic drug ratio to benefit from combined effects or combating multi-drug resistance. PLGA (poly(lactic-co-glycolic acid)) is a commonly used polymer for drug delivery systems due to its biodegradability, biocompatibility, and controlled drug release characteristics. In recent times, PLGA NPs drug delivery systems have been utilized extensively in cancer therapy. Following the unique properties of PLGA, carriers of various structures are designed to maintain the function of drugs or bioactive substances, which ensure the efficient delivery of molecules, and enhance the bioavailability of drugs in targeted tissues (Ruirui et al. 2021). Dual drug encapsulation using PLGA can be an effective strategy for lung cancer treatments. Co-delivery of PLGA allows for the controlled release of both the drugs at the same time, providing a synergistic effect and potentially reducing drug resistance. For example, in an earlier study, doxorubicin and sorafenib were combined in nanotherapeutics using PLGA, allowing the anticancer drugs to work in synergistic effects (Huang et al. 2016; Babos et al. 2018).

An appropriate composition can achieve a synergistic effect by delivering anticancer drugs to tumor cells at the same time (Wen et al. 2017). Additionally, another study has revealed that dual-drug-loaded inhalable PLGA porous NPs greatly reduced tumor development and spread in animals with in situ lung cancer (Xie et al. 2021). Considering these benefits, the current investigation focused on co-delivery of the natural compounds phytol and α-bisabolol using FDA-approved PLGA NPs as the drug delivery system. PLGA was chosen for its high biocompatibility, substantial drug-loading capacity, and potential for rapid therapeutic applications (Makadia and Siegel 2011; Rezvantalab et al. 2018).

Phytol is a diterpene alcohol found in plants such as green tea, and it has been shown to have anti-proliferative and apoptotic effects on various cancer cells, including lung cancer cells (Komiya et al. 1999; Thakor et al. 2017; Sakthivel et al. 2018). α-Bisabolol is a natural terpene alcohol found in chamomile and other plants, and it has been shown to have an anti-proliferation effect on A549 cells (Cavalieri et al. 2004; Murata et al. 2017; Wu et al. 2018). Furthermore, it has been suggested that the inclusion of α-bisabolol into PLGA NPs is a possible approach for creating novel anti-inflammatory, antipyretic, and perhaps immune therapeutic substances (Marongiu et al. 2014). In addition to that, the inclusion of both the A549 (NSCLC cell line) and L-132 cell line, a normal human alveolar cell line in the study, facilitated a comparative analysis between cancerous and normal cell lines. The utilization of L-132 cells, representing normal lung tissue, was integral for evaluating the selectivity and preferential targeting of cancer cells in lung anticancer studies.

In a prior study, the research demonstrated the synergistic induction of apoptosis and cell senescence in NSCLC cells by phytol and α-bisabolol, highlighting their effectiveness as anti-cancer agents and their potential application in the development of new therapies for lung cancer (Kiruthiga et al. 2024). The objective of the present study was to co-deliver phytol and α-bisabolol using PLGA NPs as a therapeutic approach for NSCLC. To achieve this, phytol and α-bisabolol was individually encapsulated within PLGA NPs, as well as a combination of both compounds. The NPs were characterized and their safety profile was evaluated. Furthermore, the study aimed to elucidate the apoptotic mechanisms through which the phytol and α-bisabolol-loaded PLGA NPs exerted their anti-cancer effects. The outcomes of this study have the potential to provide valuable insights into the advancement of innovative therapeutic modalities for NSCLC, particularly by exploiting the co-delivery of phytol and α-bisabolol using PLGA NPs.

Materials and methods

Cell culture and chemicals

The human adenocarcinoma lung cancer cells A549 and normal human lung epithelial cell line L-132 were obtained from the National Centre for Cell Science (NCCS) in Pune, India. The A549 and L-132 cells were cultured in DMEM medium supplemented with 10% FBS and 1× antibiotic solution (streptomycin and penicillin) at 37 °C in a humidified atmosphere with 5% CO_2. The DMEM medium was purchased from Gibco in Grand Island, USA. An Apoptosis Kit, containing Annexin V-FITC (Fluorescein isothiocyanate) and PI (Propidium Iodide), was obtained from Thermo Fisher Scientific in Waltham, MA, USA.

Experimental chemicals, including phytol, (-)-α-bisabolol, poly(d,l-lactide-co-glycolide), 5-diphenyltetrazolium bromide (MTT), dimethyl sulfoxide (DMSO), and secondary antibody (anti-mouse immunoglobulin G), were obtained from Sigma in St. Louis, MO, USA. β-Actin, B cell lymphoma 2 (Bcl-2), and Bcl-2-associated X (Bax) were purchased from Santa Cruz Biotechnology Inc. in Dallas, Texas, USA. All the chemicals used in the experiments were of high purity and high grade, obtained from HiMedia in Mumbai, MH, India.

Preparation and characterization of the formulation

Preparation of PLGA-Phy NPs, PLGA-Bis NPs, PLGA-Phy+Bis NPs

Nanoparticles containing PLGA and either phytol (PLGA-Phy), α-bisabolol (PLGA-Bis), or both phytol and α-bisabolol (PLGA-Phy+Bis) were made using the oil-in-water emulsion

solvent evaporation method (Mathew et al. 2012). In detail, 40 mg of PLGA (with a ratio of 50:50 and a molecular weight range of 30,000–60,000) was dissolved in 3 mL of dichloromethane. Subsequently, 5 mg of phytol, 5 mg of α-bisabolol, and 5 mg of both compounds were added to the solution. The mixture was stirred on a magnetic stirrer for 10 min to break down the compounds. The resulting mixtures were then added drop by drop to 20 mL of 1% polyvinyl alcohol (PVA), which was used as a surfactant to make a fine emulsion. The composite suspension of PLGA-Phy, PLGA-Bis, and PLGA-Phy+Bis underwent sonication at 40% amplitude for 5 min. The emulsion was left on the stirrer for 12 h to facilitate solvent evaporation. The nanoparticles were subsequently harvested through centrifugation at 13,000 rpm for 15 min at 4°C. Following this, the nanoparticle pellets underwent triple washing with water, were freeze-dried, and were stored at −20°C for future use. Blank nanoparticles were produced using an identical procedure, excluding the addition of phytol and α-bisabolol. For all analytical assessments, the nanoparticles were dispersed in milli-Q water.

Drug loading and encapsulation efficiency

After the synthesis of the NPs, the amount of phytol and α-bisabolol were measured following centrifugation at 13,000 rpm and 4°C for 15 min. The encapsulation efficiency (EE), drug loading capacity (DLC), and yield of the NPs were then quantified through UV analysis, as outlined in Mathew et al. (2012). To do so, a standard calibration curve was created using standard concentrations of phytol and α-bisabolol in dichloromethane, ranging from 1 to 5 mg/mL. The amount of each compound present in the NPs was measured by taking the absorbance at 250 nm for phytol and 212 nm for α-bisabolol. Finally, the EE, DLC, and yield of the NPs were calculated individually, based on the results obtained from the UV analysis.

Particle size and zeta potential

Dynamic light scattering (DLS) and micro-electrophoretic techniques were used for investigating the main physicochemical parameters of PLGA NPs such as polydispersity index (PDI), hydrodynamic diameter, and particle charge (zeta potential), on a Malvern Zetasizer Nano Series (Malvern Zetasizer Nano-ZS90, UK) equipped with a He–Ne laser (632 nm). DLS measurements were taken at 26°C with a detection angle of 175°. The mean diameter of the samples was measured in triplicate with 10–20 readings per sample and the results were expressed as mean size ± SD. When the PDI values ranged from 0.01 to 0.7, the particle distributions were narrow. High PDI readings (PDI > 0.7) showed relatively broad distributions.

High-resolution transmission electron microscope analysis

The morphology of the obtained NPs was studied by using high-resolution transmission electron microscopy (HR-TEM; Quanta FEG 250, FEI, Eindhoven, The Netherlands). For the TEM imaging, before observation, PLGA NPs were diluted 1:50 (v/v) and a few drops of diluted PLGA NPs were directly on a Cu–Ni grid and stained with uranyl acetate (2.5%) for 5 min followed by drying for 12 h at 26°C.

Characterization of drug-loaded PLGA NPs using FTIR spectroscopy

The FT-IR spectrophotometer (FTIR Thermo Nicolet 380 spectrometer) was used for the study, and the spectra were recorded in the region of 3800–500 cm^{-1} with a resolution of 2 cm^{-1}. To make the pellets, samples were mixed individually with potassium bromide (300 mg) and compressed in a hydraulic press at a pressure of 200 kg/cm^2 for 3 min. The pellets containing drug-loaded PLGA NPs were analyzed by placing the compressed pellet in the light path and recording the spectral data.

GC-MS drug release study

To evaluate the active drug content available in post-processed nanoparticle samples, each sample (PLGA-Phy, PLGA-Bis, and PLGA-Phy-Bis) was analyzed. Agilent gas chromatography (GC-MS/MS, Agilent Tech 7890B GC System) Q with a fused GC column (DB-624 [Agilent]; 30 m × 0.53 mm, 3.00 m) was used to analyze NPs. The components of the NPs were identified probably by matching peaks using NIST 17.0 libraries, and the results were verified by comparison with peaks of mass spectra reported in the published literature.

In vitro drug release kinetics

The in vitro drug release profile of PLGA-Phy+Bis NPs was studied by the dialysis method. Briefly, 1 mg of nanoparticle suspension was placed in a dialysis bag (molecular weight cutoff 10,000–12,000, Himedia, Mumbai, India), which was then sealed at both ends. The dialysis bag was soaked in 5 mL of 0.1 M phosphate-buffered saline (pH 7.4), which was stirred constantly at 100 rpm and maintained at 37°C in a shaker. At various time intervals, a sample of the solution was withdrawn, and the same volume of fresh dissolution medium was replaced in a beaker. The absorbance of the solutions was determined in triplicate using a UV spectrophotometer at 250 nm for phytol and 212 nm for α-bisabolol (Ray et al. 2017).

Biocompatibility studies

Cell viability

The cytotoxic effects of PLGA-Phy NPs, PLGA-Bis NPs, and PLGA-Phy+Bis NPs against lung cancer cell line A549 and normal human lung alveolar epithelial cell L-132 were determined by MTT assay. Cells (1×10^5/mL) were seeded per well in 96-well plate containing DMEM and incubated for 24 h. The medium was then removed and the cells were treated for 24 h with PLGA-Phy NPs, PLGA-Bis NPs, and PLGA-Phy+Bis NPs at various concentrations (0 to 100 µg/mL, 0 to 50 µg/mL, and 0 to 50 µg/mL, respectively). After removing the medium from the wells, 100 µL of MTT (1mg/mL) was added. Then, the formazan products were dissolved with dimethyl sulfoxide (DMSO) and incubated in the dark for 1 h at ambient temperature. At 570 nm, UV absorbance was measured using a multi-well plate reader (Molecular Device Spectromax M3 with Softmax Pro V5 5.4.1 software). The IC_{50} values for PLGA-Phy, PLGA-Bis, and PLGA-Phy+Bis NPs were determined by using graphpad prism.

AnnexinV-FITC/PI staining

The translocation of phosphatidylserine in cells treated with PLGA-Phy NPs, PLGA-Bis NPs, and PLGA-Phy+Bis NPs was assessed using AnnexinV-FITC and PI labeling according to the manufacturer's instructions (Invitrogen, Catalog no. V13242). Following treatment with IC_{50} concentration of PLGA-Phy, PLGA-Bis, and PLGA-Phy+Bis NPs, the cells were washed with ice-cold PBS and suspended in 1× AnnexinV binding buffer. In addition, the cells were stained with 5 µL of AnnexinV-FITC and 100 µl of the PI stain (50 µg/mL) and incubated in the dark for 15 min. After the incubation period, the cells were rinsed and resuspended in 0.5 mL of 1× Annexin V binding buffer. Subsequently, apoptotic cells were examined using fluorescence microscopy (Nikon ECLIPSE, Ti-E, Japan) with AnnexinV and PI labeling to identify positively stained cells.

Western blot

After treatment with PLGA-Phy NPs, PLGA-Bis NPs, and PLGA-Phy+Bis NPs, A549 cells per well were trypsinized and washed with PBS for analysis of the apoptotic mechanism using western blot. The pelleted cells were mixed with RIPA lysis buffer (150 mM NaCl, 1% NP-40, 0.5% sodium deoxycholate, 0.1% sodium dodecyl sulfate, 50 mMTris, pH 8.0) and 1 mM PMSF, and then incubated for 2 h at −20°C. After incubation, the cells were vortexed and centrifuged for 30 min at 13,000 rpm and 4°C. The cell-free supernatant was transferred to new tubes, and the protein content was measured using the Bradford technique. On a 12% SDS-PAGE gel, about 100g of protein was separated and then transferred to a PVDF membrane. After transformation, membranes were blocked with 5% skim milk at 4°C for 3 h, followed by overnight incubation at 4°C with appropriate primary antibodies (Bcl-2, Bax, and β-actin (Internal control) at a dilution of 1:1000). After incubation, membranes are washed with TBST (Tris-buffered saline with Tween 20) for 5 min, then incubated for 3 h at 4°C with an anti-mouse ALP-conjugated secondary antibody (1:1000). The proteins were visualized using 5-bromo-4-chloro-3-indolyl phosphate (BCIP) and nitro blue tetrazolium (NBT), and pictures were acquired using a gel documentation system. Quantification of the protein bands was performed using ImageJ software.

In vivo toxicity assessment

The toxicity assessment was conducted using zebrafish embryos (*D. rerio*), following ethical approval from the Institutional Animal Ethics Committee (IAEC/AU/OCT/2021/Fish-6). The embryos were harvested from the zebrafish aquarium tank at 3 h post-fertilization (hpf) and transferred to 24-well plates, with each well containing 30 embryos and an exposure medium. The toxicity assessment of the NPs was carried out following the standard protocol (Lammer et al. 2009). The zebrafish embryos were treated with different concentrations of NPs including PLGA-Phy NPs (50 and 100 µg/mL), PLGA-Bis NPs (50 and 100 µg/mL), and PLGA-Phy+Bis NPs (50 and 100 µg/mL). Each test concentration was performed in triplicate at various time intervals (24, 48, 72, and 96 hpf), and morphological abnormalities were examined using an OLYMPUS CH 20i inverted-phase contrast light microscope. The mortality results were then calculated.

Statistics

The experiments were performed in triplicate ($n = 3$) and statistical analysis was conducted using IBM SPSS Statistics (version 25). To determine the IC_{50} value, GraphPad Prism 7.04 software (La Jolla, USA) was employed. One-way ANOVA was used to analyze the statistical variance between the control and treated groups. To identify significant differences between the control and treatment groups, the Dunnett T3 post hoc test was applied, with a p-value less than 0.05 being considered significant.

Results

Preparation and characterization of phytol, α-bisabolol, and their combination in PLGA NPs

In the current study, phytol, α-bisabolol, and their combinations were successfully encapsulated into PLGA NPs by the oil-in-water immersion, solvent evaporation method (Fig. 1). The results showed that the drug/polymer ratio of 1:4 for phytol and α-bisabolol resulted in nearly 83.30 ± 0.81% and 77.17 ± 0.181% encapsulation efficiency (EE), respectively. PLGA-Phy+Bis NPs with a drug/polymer ratio of 0.5:0.5:4 (phytol:α-bisabolol:PLGA) resulted in nearly 82.64 ± 0.09% and 78.71 ± 0.103% EE, respectively. These findings suggest that the encapsulation process improves the solubility of phytol and influences its physicochemical and pharmacokinetic properties (Sah et al. 2017). The high EE of Phy-PLGA, Bis-PLGA, and PLGA-Phy+Bis NPs observed in the study can be attributed to the ionic interactions between the drug and the polymer. Moreover, it reduces the wastage of drugs during the encapsulation process.

Furthermore, the loading efficiency of PLGA-Phy, PLGA-Bis, and PLGA-Phy+Bis NPs were found to be 8.49 ± 0.08%, 8.64 ± 0.02%, and 8.43 ± 0.01% (phytol), 8.026 ± 0.005% (α-bisabolol), respectively, depending on the drug/polymer ratio. During the formulation process, an increase in the drug concentration was observed to increase the loading efficiency. This effect might be due to the ability of the polymer matrix to accommodate a higher amount of phytol and α-bisabolol molecules in the polymeric matrix, thus ensuring the ability of the polymeric matrix to release higher drug concentrations at the specific target site. The yield of the NPs was around 80%. Notably, the high EE, loading efficiency, and yield of the NPs achieved in this study (Table 1) are similar to those reported in previous studies on PLGA NPs (Fornaguera et al. 2015).

Nanocarrier size, polydispersity, and particle charge

Photon correlation spectroscopy (PCS) was employed to determine the mean particle size of drug-loaded PLGA NPs. The analysis revealed that the NPs, which were prepared with three different drug compositions (phytol, α-bisabolol, and phytol+α-bisabolol) and incorporated into PLGA, fell within the nanometer range. The mean size of PLGA-Phy NPs, PLGA-Bis, PLGA-Phy+Bis NPs, and PLGA NPs alone was found to be 162.5 ± 12.33 nm, 137.3 ± 7.79 nm, 189.3 ± 5 nm, and 91.1 ± 1.9 nm, respectively, as confirmed by DLS measurements. The size distributions of all

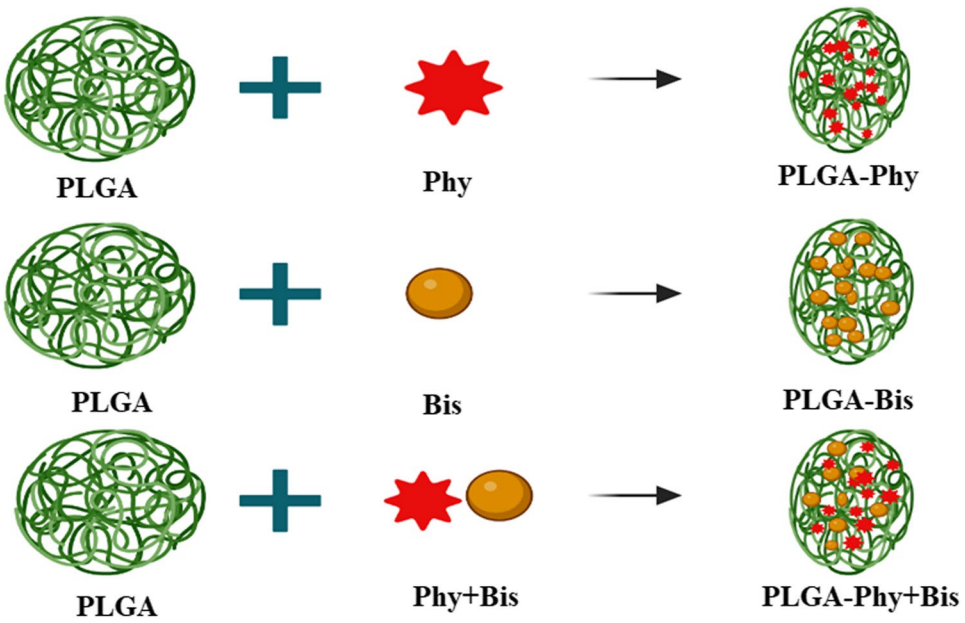

Fig. 1 A diagram illustrating the encapsulation of bioactive compounds within PLGA nanoparticles, including PLGA-Phy NPs, PLGA-Bis NPs, and PLGA-Phy+Bis NPs

Table 1 Encapsulation efficiency, Loading efficiency, and Yield

NPs	Encapsulation efficiency (%)		Loading efficiency (%)	Yield (%)
PLGA-Phy NPs	83.30 ± 0.81		8.49 ± 0.08	74.23 ± 3.87
PLGA-Bis NPs	77.17 ± 0.181		8.64 ± 0.02	70.24 ± 2.24
PLGA-Phy+Bis NPs	Phy	82.64 ± 0.09	8.43 ± 0.01	72.46 ± 2.64
	Bis	78.71 ± 0.103	8.026 ± 0.005	

nanoparticle formulations ranged from 0.224 to 0.348, as shown in Table 2 and Fig. 2a. The mean zeta potential of PLGA-Phy NPs, PLGA-Bis, and PLGA-Phy+Bis NPs was determined by Malvern zeta-sizer and it was found to be −38.2mV, −0.3 mV, and 0.1 mV, respectively.

Shape and morphology

The study used high-resolution transmission electron microscopy (HR-TEM) to characterize the PLGA-stabilized NPs. HR-TEM is a rapid, efficient, and generally non-invasive approach that may offer evidence on the form, morphology, and size distribution of polymeric nano-systems. The TEM imaging revealed oval-shaped particles of equally uniform size across the sampling region. The darkest area corresponds to the thicker PLGA outer shell, suggesting that these shells were created effectively. The size obtained was 318±27 nm, 144±25 nm, and 268 ±54 nm for PLGA-Phy, PLGA-Bis, and PLGA-Phy+Bis NPs respectively (Fig. 2a).

Table 2 Particle size, polydispersity index, charge and electrical mobility mean of PLGA-loaded nanoparticles

	Particle size (nm) ± SD	Polydispersity index	Charge (mV)	Electrical mobility mean (cm/Vs)
PLGA-Phy	162.5 ± 12.33 nm	0.312	−38.2	−0.000196
PLGA-Bis	137.3 ± 7.79 nm	0.348	−0.3	−0.000001
PLGA-Phy+Bis	189.3 ± 5 nm	0.224	0.1	0.000001

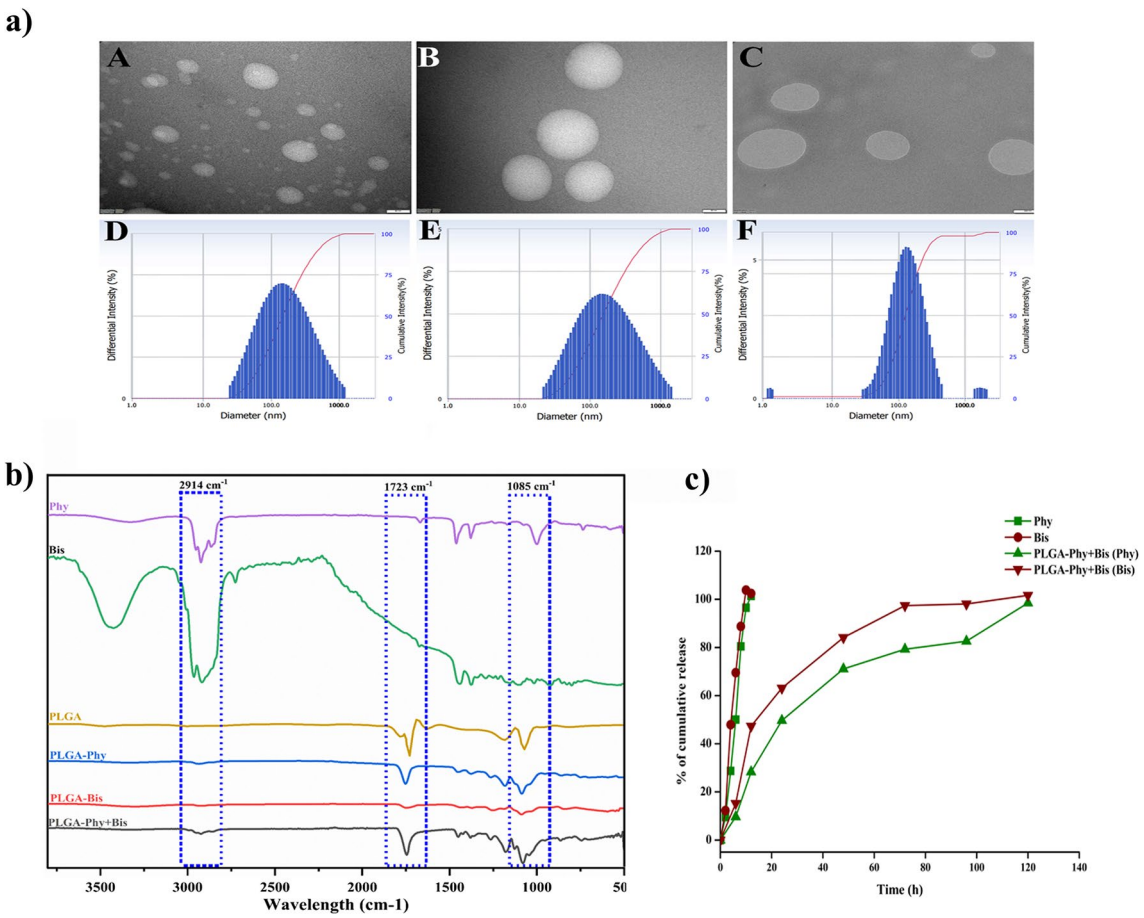

Fig. 2 (**a**) High-resolution transmission electron microscopy image of (**A**) PLGA-Phy NPs, (**B**) PLGA-Bis NPs, (**C**) PLGA-Phy+Bis NPs and the size distributions of all NPs by DLS measurements, (**D**) PLGA-Phy NPs, (**E**) PLGA-Bis NPs, (**F**) PLGA-Phy+Bis NPs. (**b**) FT-IR spectra of phytol, α-bisabolol, PLGA NPs alone, PLGA-Phy NPs, PLGA-Bis NPs, and PLGA-Phy+Bis NPs. (**c**) In vitro drug release profile of phytol, α-bisabolol, and PLGA-Phy+Bis NPs

FTIR spectroscopy analysis of drug-loaded PLGA NPs

The chemistry of drug-loaded PLGA NPs was assessed using Fourier transform infrared (FTIR) vibrational spectroscopy. As shown in Fig. 2b, the FTIR spectra of PLGA, phytol, α-bisobolol, and NPs including PLGA-Phy, PLGA-Bis, and PLGA-Phy+Bis depict spectra derived from the IR studies, which correspond to wavelengths of 3800 cm^{-1} to 500 cm^{-1}, respectively. The FTIR spectra of PLGA reveal distinctive peaks due to the functional groups included in it. The carbonyl stretching vibration in the –COO– group, which is present in both the lactic and glycolic acid monomers, generates a peak close to 1723 cm^{-1}. The C–H bending vibration in the $–CH_3$ found in the lactic acid monomer and glycolic acid monomer causes the peak at about 1402 cm^{-1} and 1187 cm^{-1}, respectively (Soni et al. 2010). The C–O–C stretching vibration in the COO group is responsible for the peak near 1085 cm^{-1}. The C–H bending vibration in the CH_2 group found in the PLGA backbone essentially creates the peak around 1450 cm^{-1} (Soni et al. 2010).

Free drugs Phy and Bis exhibit absorption peaks at 2928, 1469, 1375, and 1000 cm^{-1} (Wang et al. 2013) and 3431, 2912, 1447, 1370, and 1011 cm^{-1} (Picquart and Lefèvre 2003), respectively. All the groups on Phy and Bis are highly related to the presence of –OH, C–H, and C=O groups. The main peaks of PLGA at 2914, 1723, and 1085 cm^{-1} can be attributed to –COO, $–CH_3$, and C–O groups, respectively. The spectral analysis for PLGA-Phy, PLGA-Bis, and PLGA-Phy+Bis indicates that the functional groups on the surface of the PLGA NPs have chemical characteristics similar to the PLGA. As seen on the FTIR spectra, there was no chemical interaction between functional groups of PLGA and drug actives, indicating the structural stability upon nanoparticle synthesis with Phy and Bis. The interaction study between the drug and polymer was evaluated. The absence of distinctive spectra in the PLGA-Phy, PLGA-Bis, and PLGA-Phy+Bis indicates that drug actives and PLGA were not involved in intermolecular interaction. However, the intensity of the peak at 2914, 1723, and 1085 cm^{-1} was decreased in the FTIR spectrum of the PLGA-Phy+Bis NPs (Anwer et al. 2019). The decrease in peak intensity following nano-PLGA encapsulation is an instant of encapsulation efficiency. Upon encapsulation within a polymeric matrix, both molecules and the surrounding polymer modify their vibrational modes, resulting in a diminished intensity of characteristic peaks in FTIR spectra. Furthermore, the encapsulation process can prompt alterations in the molecular environment of the encapsulated compound, potentially introducing steric hindrance or modifying the electrostatic surroundings. These changes can impact the vibrational properties of the compound, consequently influencing the observed intensity of FTIR peaks (Hadjiivanov et al. 2021).

GC-MS drug release study

The chemical composition of PLGA nanocarriers loaded with drugs was analyzed using GC-MS, by measuring peak areas and retention times (Fig. 3 and Table 3). The retention time for phytol was found to be the highest at 20.7373 s, while α-bisabolol was detected at 16.53 s in all NPs. The GC-MS analysis showed that PLGA-Phy contained 57.22% phytol, while PLGA-Bis contained 87.54% α-bisabolol. The higher drug encapsulation efficiency of α-bisabolol in PLGA-Bis led to an increase in particle size compared to PLGA-Phy. In PLGA-Phy+Bis, 38.02% of phytol and 64.72% of α-bisobolol were found to be encapsulated when compared individually. α-Bisabolol was identified as the major drug encapsulated in both PLGA-Bis and PLGA-Phy+Bis.

In vitro drug release kinetics

The in vitro drug release kinetics of PLGA-Phy+Bis NPs were evaluated using the dialysis method, where the percentage of phytol and α-bisabolol released from the PLGA NPs at various time intervals was analyzed. The release rate of a drug from a nanocarrier depends on several factors such as the concentration of PLGA, size of the nanoparticle, solubility, molecular weight, and biodegradable properties of the polymer matrix (Jinhyun Hannah Lee and Yeo 2016). The resulting PLGA-Phy+Bis NPs showed sustained release behavior, with a slow cumulative drug release of up to 98.4% from the NPs (drug 1: drug 2:polymer ratio, 0.5:0.5:4) observed over 120 h (Fig. 2c). The encapsulated NPs were completely released within this time frame. Similar to other loaded PLGA NPs, a biphasic release pattern with an initial burst effect followed by sustained drug release was observed (Fornaguera et al. 2015). Overall, the in vitro drug release study demonstrated that the delivery action of PLGA-Phy+Bis NPs sustained the release of phytol and α-bisabolol molecules, making them a promising candidate for the treatment of NSCLC.

Anti-cancer activity assessement through MTT assay

The PLGA-Phy, PLGA-Bis, and PLGA-Phy+Bis NPs significantly inhibited the proliferation of A549 cells in a concentration dependent manner. In PLGA alone, NPs do not exhibit any inhibition on A549 cells. The IC_{50} values of PLGA-Phy, PLGA-Bis, and PLGA-Phy+Bis against A549 cells were found to be 25 µg/mL, 14.56µg/mL, and 14 µg/mL at 24 h respectively (Fig. 4a). Overall, the MTT results confirmed that the PLGA-Phy+Bis NPs have a significant anti-proliferative effect against A549 cells.

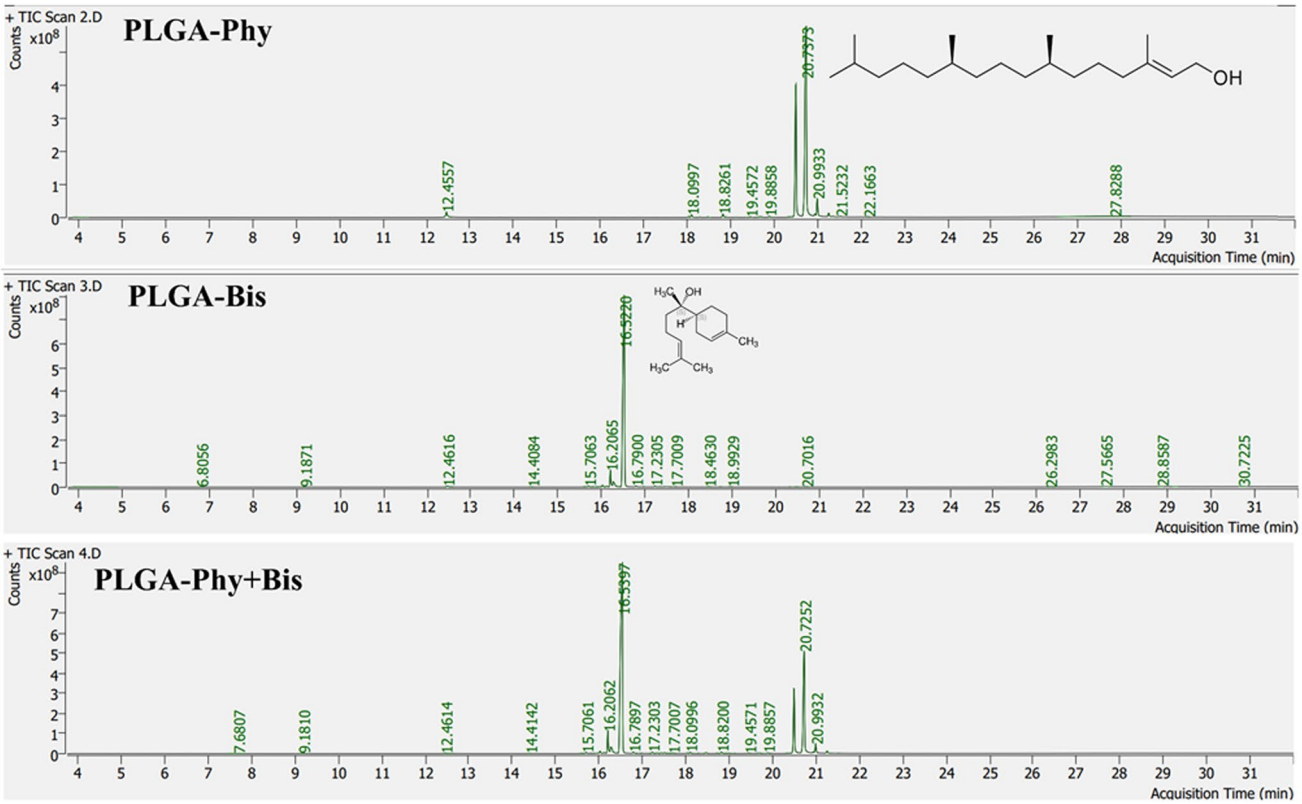

Fig. 3 GC-MS drug release analysis of all NPs

Table 3 Drug release profile of NPs analyzed by GC-MS

	PLGA-Phy	PLGA-Bis	PLGA-Phy+Bis Phy	PLGA-Phy+Bis Bis
Drug Area	1629527024	2241923580	1203885637	3135267431
Total Area	2847620700	2560981157	5534069013	5534069013
% availability	57.22	87.41	21.75	56.65
			78.40	
		% less drug in PLGA-Phy+Bis (comparing single)	38.01	64.72

Apoptotic assessment through AnnexinV-FITC/PI staining and western blot analysis

Apoptotic cells display a signal that presumably exposes phosphatidylserine to the outer cell membrane. In addition, apoptotic cells lose their membrane integrity because proteolytic enzymes such as caspase are activated. To examine the apoptosis induced by PLGA-Phy NPs, PLGA-Bis NPs, and PLGA-Phy+Bis NPs, AnnexinV-FITC, and PI staining were performed and analyzed by fluorescence microscopy. A549 cells were treated for 24 h with IC_{50} concentrations of PLGA-Phy NPs, PLGA-Bis NPs, and PLGA-Phy+Bis NPs, and the percentage of apoptotic cells was quantified using Annexin V-FITC and PI. Under fluorescence microscopy, AnnexinV-FITC and PI-positive cells upon exposure to PLGA-Phy NPs, PLGA-Bis NPs, and PLGA-Phy+Bis NPs were initially qualitatively observed. The increase of Annexin V and PI-positive cells was confirmed by fluorescence images shown in Fig. 4b.

Furthermore, the quantitative analysis revealed a significant and substantial increase in both early and late apoptotic cells following exposure to PLGA-Phy NPs, PLGA-Bis NPs, and PLGA-Phy+Bis NPs (Fig. 4c). Notably, PLGA-Phy+Bis NPs exhibited a higher proportion of late apoptotic cells compared to PLGA-Phy NPs and PLGA-Bis NPs. These findings strongly support the notion that PLGA-Phy NPs, PLGA-Bis NPs, and PLGA-Phy+Bis NPs actively promote apoptotic cell death in A549 cells.

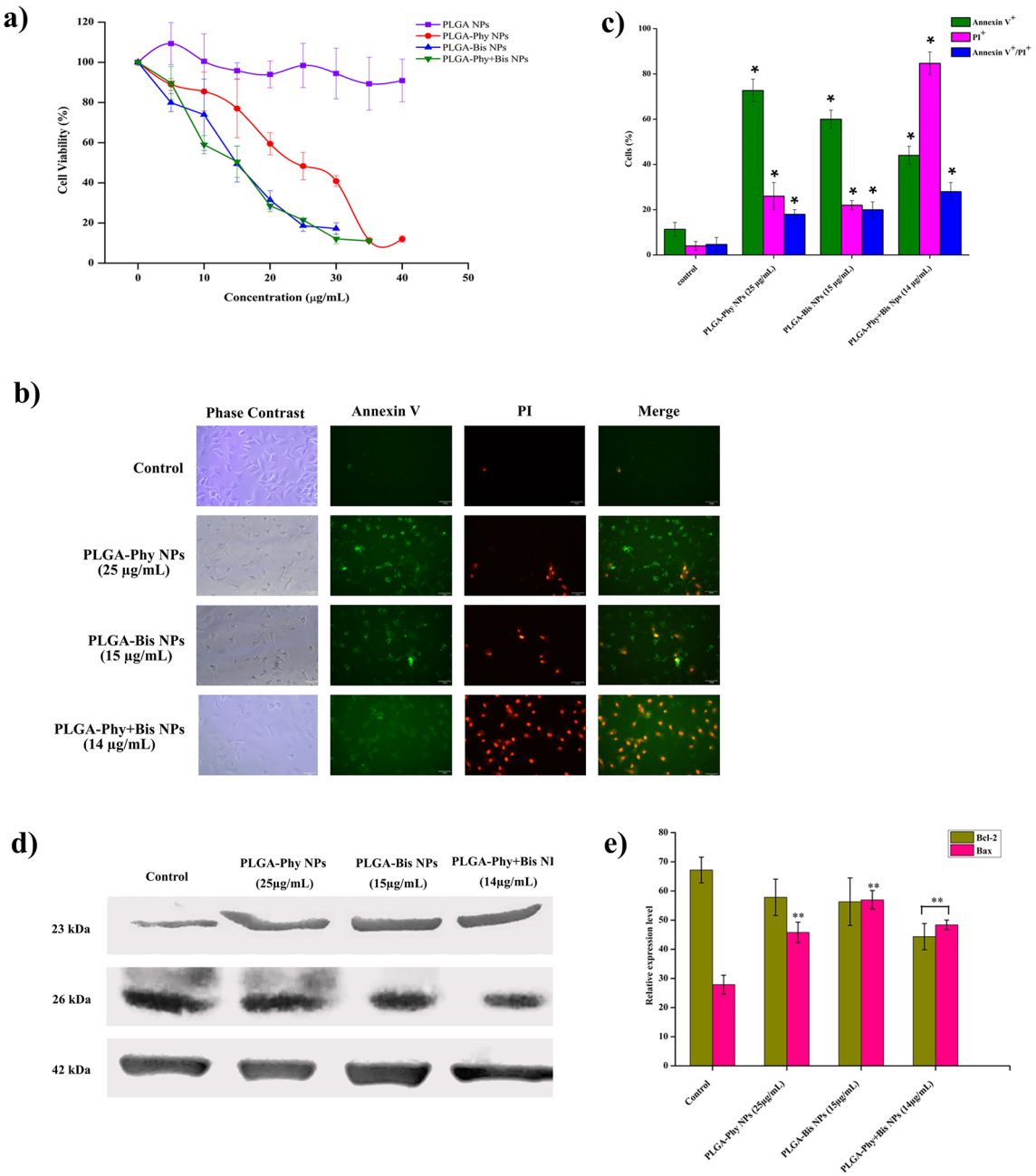

Fig. 4 PLGA-Phy+Bis NPs bioactivity against A549 cells. **a** Antiproliferative effect of PLGA-Phy NPs, PLGA-Bis NPs, and PLGA-Phy+Bis NPs against A549 cells. **b** Representative microscopic images of A549 cells for apoptosis study using Annexin V-FITC/PI staining. **c** Quantitative measurement of Annexin V/PI positive apoptotic cells after treatment with all NPs for 24 h. Data are presented as the mean ± SD of three samples per group. **d** Western blot analysis of Bax and Bcl-2 expression in A549 cells after 24 h of incubation with all NPs at IC_{50} concentrations. The gel blots were cropped from different gel and full length of blot is given in supplementary file. **e** Changes in the protein expression levels of apoptotic regulators in A549 cells treated with all NPs. The protein levels were normalized with β-actin. (*P<0.05 & **P<0.01 vs control group)

To investigate the underlying biochemical processes associated with the induction of apoptosis, western blot was employed to analyze the expression levels of key apoptotic proteins. In particular, the anti-apoptotic protein Bcl-2 and the pro-apoptotic protein Bax were assessed. The results revealed a significant reduction in Bcl-2 expression and a concurrent increase in Bax expression following treatment with PLGA-Phy NPs, PLGA-Bis NPs, and PLGA-Phy+Bis NPs. Importantly, PLGA-Phy+Bis NPs exhibited a particularly pronounced reduction in Bcl-2 expression

and upregulation of Bax, as depicted in Fig. 4d and e. This alteration in apoptotic protein expression strongly suggests that these NPs induce apoptotic cell death as the predominant mode of cell death.

In vitro and in vivo safety assessment

The effects of PLGA-Phy, PLGA-Bis, and PLGA-Phy+Bis on the safety of human L-132 cells were investigated using the MTT test. The tested NPs did not affect the growth and viability of normal human lung L-132 cells after exposure for 24 h. However, mild toxicity was observed at the maximal dose of 200 µg/mL in PLGA-Phy and PLGA-Bis at 24 h, as shown in Fig. 5a, compared to PLGA-Phy+Bis. Cytotoxic studies conducted on normal human cells revealed that the combination of Phy and Bis selectively induced cell death in A549 cells alone without affecting the normal cells.

The in vivo safety of PLGA-Phy NPs, PLGA-Bis NPs, and PLGA-Phy+Bis NPs was evaluated by observing the morphology and mortality of zebrafish embryos at different concentrations (50 µg/mL and 100 µg/mL) and time intervals (24, 48, 72, and 96 hpf). No mortality or morphological abnormalities were observed even after 96 hpf at a higher concentration of 100 µg/mL in PLGA-Phy NPs, PLGA-Bis NPs, or PLGA-Phy+Bis NPs, and their morphology resembled that of the control group (Fig. 5b). These results indicate that concentrations of up to 100 mg/L of PLGA-Phy NPs, PLGA-Bis NPs, and PLGA-Phy+Bis NPs are safe for use.

Discussion

Phytol and α-bisabolol are natural compounds with numerous pharmacological properties. However, the utility of phytol is greatly restricted due to its hydrophobic nature, which results in poor solubility in biological fluids. This problem can be overcome through encapsulation. The present study evaluated the potential of PLGA-Phy+Bis NPs as a drug delivery system for the treatment of NSCLC. Phytol, α-bisabolol, and their combination were successfully encapsulated into PLGA NPs by the oil-in-water immersion, solvent evaporation method. The high encapsulation efficiency of PLGA-Phy+Bis NPs could be attributed to the ionic interactions between the drug and the polymer. Therefore, the utilization of ionic interactions for encapsulating phytol and α-bisabolol proves to be an effective strategy in minimizing drug wastage during the encapsulation process (Singh and Tiwari 2010). Previous research has highlighted the significance of this ratio in

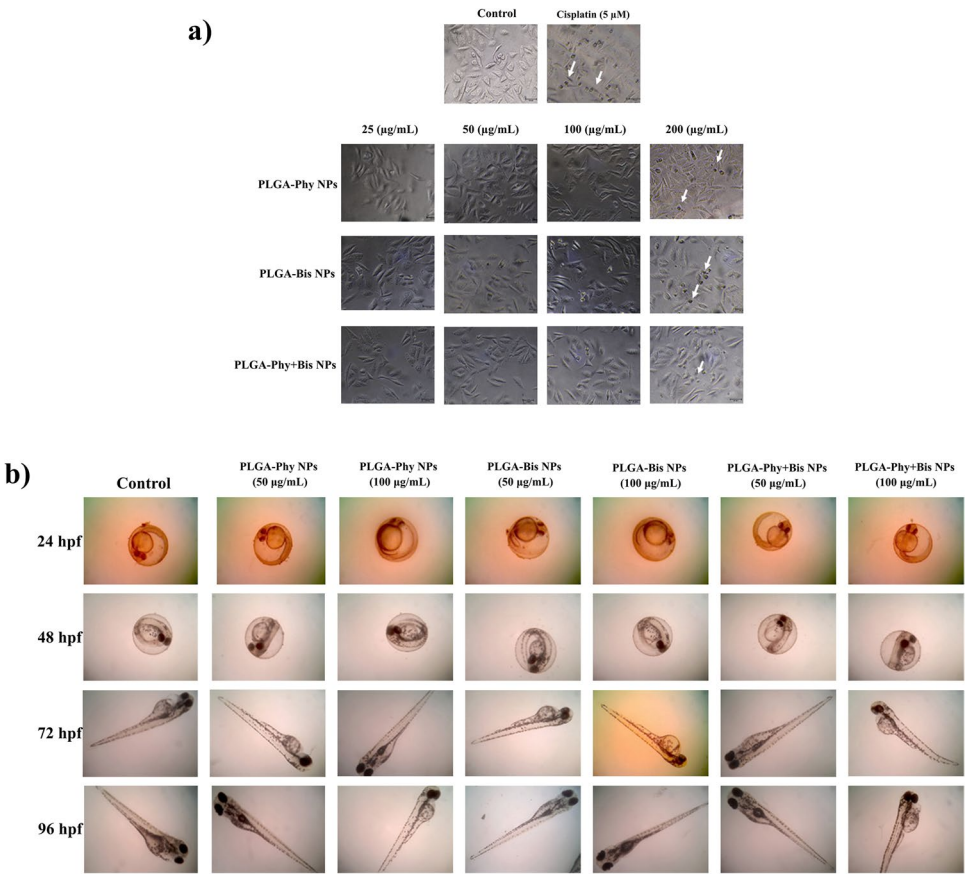

Fig. 5 Toxicity assessment of all NPs: **a** Microscopic images of normal lung L-132 cells treated with specified concentrations (25, 50, 100, and 200 µg/mL) of PLGA-Phy NPs, PLGA-Bis NPs, and PLGA-Phy+Bis NPs after 24 h. **b** Toxic effects of PLGA-Phy NPs, PLGA-Bis NPs, and PLGA-Phy+Bis NPs on the development of zebrafish (*Danio rerio*) embryos. Representative pictures of each stage of embryo development at various NPs concentrations (50 and 100 µg/mL). Data are presented as the mean ± SD of three samples per group

optimizing the encapsulation efficiency of drugs within the PLGA NPs. By carefully adjusting the drug/polymer ratio, researchers were able to maximize the amount of drug incorporated into the NPs. Additionally, the drug/polymer ratio has a direct impact on the drug release characteristics of the PLGA NPs (Bala et al. 2004; Makadia and Siegel 2011). The loading efficiency of PLGA-Phy, PLGA-Bis, and PLGA-Phy+Bis NPs depended on the drug/polymer ratio, with an increase in the drug concentration leading to higher loading efficiency. This effect might be due to the ability of the polymer matrix to accommodate a higher amount of phytol and α-bisabolol molecules in the polymeric matrix, thus ensuring the ability of the polymeric matrix to release higher drug concentrations at the specific target site. The results notably highlight that the preferential encapsulation of α-bisabolol over phytol, even at equal concentrations, is attributed to its distinctive hydroxyl group arrangement, fostering a more favorable interaction with the PLGA polymer. Due to the high polarity and presence of hydroxyl groups, α-Bisabolol is highly soluble in the PLGA solution, which enhances its effective dissolution and subsequent encapsulation. Consistent computational predictions from ESOL Prediction, Ali Prediction, and SILICOS-IT reinforce this observation, affirming α-bisabolol's superior solubility compared to phytol. Furthermore, the observed differential diffusion rates in the PLGA solution suggest that α-bisabolol may exhibit a greater ability to rapidly diffuse into the PLGA polymer matrix compared to phytol, thereby contributing to the observed higher encapsulation efficiency.

The size of all nanoparticle formulations were in the nanometer range with a very narrow PDI, and the hydrodynamic diameter of the NPs fell into the region of NPs. The particle size distribution analysis for PLGA-Phy, PLGA-Bis, and PLGA-Phy+Bis revealed a narrow size distribution profile with very low PDI and high stability, which are important characteristics for effective drug delivery and passive targeting of cancer tumors, including NSCLC (Anwer et al. 2019). The small size of the NPs allows them to passively accumulate in the tumor tissues via the enhanced permeability and retention (EPR) effect, which is a common phenomenon observed in most solid tumors (Varani et al. 2020; Ibrahim et al. 2020). The high stability of the NPs ensures that they remain intact in the bloodstream and can effectively deliver the drug payload to the tumor site (Wei et al. 2016). Furthermore, the ability of the NPs to encapsulate and deliver drugs such as phytol and α-bisabolol to the tumor site has potential therapeutic benefits for NSCLC treatment. Studies have shown that both phytol and α-bisabolol have anti-cancer properties and can inhibit the growth and proliferation of NSCLC cells in multiple pathways. In a previous report, it was demonstrated that phytol and α-bisabolol synergistically inhibit A549 cells through several mechanisms, including an increase in ROS, changes in [Ca2+]i, induction of G0/G1 cell cycle arrest and cellular senescence, and intrinsic mode of apoptosis. Additionally, they may interact with the actin cytoskeleton to impede cell migration, demonstrating their potential as anti-metastatic agents (Kiruthiga et al. 2024). The zeta potential of the drug-loaded NPs exhibited negative values for PLGA-Phy (highly negative) and PLGA-Bis (near neutral), and neutral for PLGA-Phy+Bis NPs. Because of the neutral charge of PLGA-Phy+Bis, there is no electrostatic hindrance in drug-cell interactions, and it can be further used as a potent drug delivery system for multiple cancer targets. Additionally, unlike cationic and anionic nano-emulsions, neutral NPs will not accumulate in the liver and cause further toxicity. Furthermore, neutrally charged NPs do not undergo electrostatic moments (electrical mobility mean, 0.000001 cm/Vs) inside tissues, and thus can be used as a targeted delivery system via injections on the site of a tumor (Yao et al. 2019). However, some studies have shown that negatively charged NPs can improve cellular uptake and drug delivery to cancer cells due to the interaction with positively charged cell membranes (Clogston and Patri 2011). On the other hand, the near-neutral zeta potential of PLGA-Bis NPs and the neutral zeta potential of PLGA-Phy+Bis NPs may provide a balanced approach, with improved stability and reduced aggregation, while also facilitating cellular uptake and drug delivery to cancer cells due to a lack of electrostatic repulsion or attraction (Huang et al. 2016).

Although all PLGA NPs have a similar oval shape, variations in size were observed within the nanoparticles. The largest size nanoparticle on average mean size was observed in the case of individual nano-carrier PLGA-Phy, whereas PLGA-Bis had the lowest average mean size. This could be attributed to different parameters such as drug encapsulation efficiency of PLGA, molecule accepting groups in the PLGA, and chemical composition/molecular weight of phytol ($C_{20}H_{40}O$/296.5) and α-bisabolol ($C_{15}H_{26}O$/222.37) (Asal et al. 2022).

The study did not observe any form of aggregation in any of the NPs, indicating the stability and enhanced shelf life of NPs at room temperature. However, it should be noted that since TEM was performed in dry circumstances, the processed NPs had a propensity to shrink, resulting in the loss of their main shape and size, and the nanoparticle size range was less than the size distribution obtained by the DLS as provided in Table 2. Overall, the HR-TEM analysis provided valuable insights into the morphology and size distribution of the PLGA-stabilized NPs.

The dialysis method is a widely used technique to study drug release from NPs as it mimics the diffusion process that occurs in vivo (Patra et al. 2018; Weng et al. 2020). The results showed that sustained release behavior exhibited by

the PLGA-Phy+Bis NPs is an important characteristic of a drug delivery system, as it ensures that the drug is released over a longer period time, thereby increasing its efficacy. The sustained release behavior of PLGA-Phy+Bis NPs is due to the biodegradable and biocompatible properties of PLGA, which degrades gradually to release the drug at a controlled rate. The addition of phytol and α-bisabolol to PLGA NPs could have enhanced this behavior by interacting with the polymer and influencing the degradation rate (Rezvantalab et al. 2018). The anti-proliferative effect of the NPs against A549 cells suggests that these NPs have potential as therapeutic agents for NSCLC. Furthermore, the induction of apoptotic cell death by PLGA-Phy NPs, PLGA-Bis NPs, and PLGA-Phy+Bis NPs confirms their potential as a treatment option for NSCLC. The upregulation of Bax and downregulation of Bcl-2 in A549 cells treated with PLGA-Phy+Bis NPs suggests that this combination of NPs may induce apoptosis in cancer cells via the mitochondrial pathway(Balan et al. 2021). Induction of apoptosis holds significant importance in cancer therapies as it aims to eliminate cancer cells by triggering their programmed cell death (Hanahan and Robert A 2017; Chirumbolo et al. 2018). The ability of PLGA-Phy NPs, PLGA-Bis NPs, and PLGA-Phy+Bis NPs to induce apoptosis in cancer cells, as evidenced by their anti-proliferative effects and modulation of apoptotic proteins, highlights their potential as therapeutic agents for combating NSCLC. The study demonstrates that concentrations of PLGA-Phy, PLGA-Bis, and PLGA-Phy+Bis NPs up to 100 µg/mL are safe for use, as tested on L-132 cells. Notably, at a maximal concentration (200 µg/mL), both PLGA-Phy and PLGA-Bis exhibited mild toxicity at the 24 h time point, as depicted in Fig. 5a. This observed mild toxicity was significantly alleviated in the case of PLGA-Phy+Bis, underscoring the potential synergistic or protective effects arising from the combination of phytol and α-bisabolol. Furthermore, the PLGA-Phy+Bis NPs showcased a selective anti-proliferation effect in A549 cancer cells, with a notable sparing effect on normal L-132 cells. This substantiates that the safety profile of the NPs aligns with the non-toxic nature of phytol and α-bisabolol, particularly with a higher affinity for L-132 cells over A549 cells (Sakthivel et al. 2018). This finding is an important aspect of drug development as it suggests that these NPs have a low toxicity profile and can be a potential strategy for inducing apoptosis in cancer cells without affecting normal cells. These findings are consistent with previous studies reported in the literature (Rajavel et al. 2017, 2018). This is a promising finding for further development of these NPs as a drug delivery system for NSCLC, as it suggests that they may have a low toxicity profile in vivo. However, further research is needed to determine the molecular mechanism of these NPs in cancer therapy. Overall, these findings suggest that PLGA-Phy+Bis NPs hold promise as an effective and safe drug delivery system for the treatment of NSCLC.

Conclusion

In conclusion, the co-delivery of biocompatible PLGA NPs offers a promising strategy to enhance the effectiveness of therapy and minimize side effects in the treatment of NSCLC. The successful encapsulation of phytol, α-bisabolol, and their combination within PLGA NPs demonstrates their remarkable efficiency in terms of encapsulation, loading, and yield, as well as their uniform size distribution and stability. PLGA NPs exhibit significant potential as drug-delivery vehicles for lung cancer treatment, offering advantages such as improved therapeutic efficacy and reduced toxicity. By utilizing the capabilities of PLGA NPs, the delivery, and targeting of anti-cancer agents can be optimized, potentially leading to more effective and safer treatment outcomes for NSCLC patients. However, further research and development are needed to optimize the performance and application of PLGA NPs in the field of lung cancer therapy.

Supplementary Information The online version contains supplementary material available at https://doi.org/10.1007/s00210-023-02935-2.

Acknowledgements The authors thankfully acknowledge DST-FIST (Grant No. SR/FST/LSI-639/2015(C)), UGC-SAP (Grant No.F.5-1/2018/DRSII (SAP-II)), DST-PURSE (Grant No. SR/PURSE Phase 2/38 (G)), and ICMR Ad-hoc project (ISRM/Ad-hoc/31/2020-21), for providing Instrumentations and lab facilities. The authors also thank RUSA 2.0 (F. 24-51/2014-U, Policy (TNMulti-Gen), Dept of Edn, GoI).

Author contributions CK designed and conducted the experiments, with assistance from DJB in developing the methodology. SKP and NHP provided support in interpreting FTIR and GC-MS results. KPD encouraged CK to explore the topic and supervised the research findings. SJ contributed to sample preparation, while NMP and MM aided in assessing embryo toxicity. CK and KPD thoroughly reviewed the findings and jointly approved the final version of the manuscript. The authors declare that all data were generated in-house and that no paper mill was used.

Data availability The article contains all relevant data from the study. The original contributions are available upon request to the corresponding author for further inquiries.

Declarations

Ethical approval The zebrafish embryo acute toxicity test was conducted following the guidelines and regulations of the Institutional Ethics Committee of Alagappa University, Karaikudi, India. The study was approved under the ethical approval number IAEC/AU/OCT/2021/Fish-6.

Competing interests The authors declare no competing interests.

References

Anwer K, Mohammad M, Ezzeldin E et al (2019) Preparation of sustained release apremilast-loaded PLGA nanoparticles: in vitro characterization and in vivo pharmacokinetic study in rats. Int J Nanomed 14:1587–1595. https://doi.org/10.2147/IJN.S195048

Asal HA, Shoueir KR, El-Hagrasy MA, Toson EA (2022) Controlled synthesis of in-situ gold nanoparticles onto chitosan functionalized PLGA nanoparticles for oral insulin delivery. Int J Biol Macromol 209:2188–2196. https://doi.org/10.1016/j.ijbiomac.2022.04.200

Babos G, Biró E, Meiczinger M, Feczkó T (2018) Dual drug delivery of sorafenib and doxorubicin from PLGA and PEG-PLGA polymeric nanoparticles. Polymers (Basel) 10:895. https://doi.org/10.3390/polym10080895

Bala I, Hariharan S, Kumar MR (2004) PLGA nanoparticles in drug delivery: the state of the art. Crit Rev Ther Drug Carrier Syst 21:387–422. https://doi.org/10.1615/CritRevTherDrugCarrierSyst.v21.i5.20

Balan DJ, Rajavel T, Das M et al (2021) Thymol induces mitochondrial pathway-mediated apoptosis via ROS generation, macromolecular damage and SOD diminution in A549 cells. Pharmacol Reports 73:240–254. https://doi.org/10.1007/s43440-020-00171-6

Cavalieri E, Mariotto S, Fabrizi C et al (2004) α-Bisabolol, a nontoxic natural compound, strongly induces apoptosis in glioma cells. Biochem Biophys Res Commun 315:589–594. https://doi.org/10.1016/j.bbrc.2004.01.088

Chirumbolo S, Bjørklund G, Lysiuk R et al (2018) Targeting cancer with phytochemicals via their fine tuning of the cell survival signaling pathways. Int J Mol Sci 19:3568. https://doi.org/10.3390/ijms19113568

Clogston JD, Patri AK (2011) Zeta potential measurement. In: Methods in Molecular Biology. pp 63–70

Fornaguera C, Feiner-Gracia N, Calderó G et al (2015) Galantamine-loaded PLGA nanoparticles, from nano-emulsion templating, as novel advanced drug delivery systems to treat neurodegenerative diseases. Nanoscale 7:12076–12084. https://doi.org/10.1039/C5NR03474D

Gavas S, Quazi S, Karpiński TM (2021) Nanoparticles for cancer therapy: current progress and challenges. Nanoscale Res Lett 16:173. https://doi.org/10.1186/s11671-021-03628-6

Hadjiivanov KI, Panayotov DA, Mihaylov MY et al (2021) Power of infrared and raman spectroscopies to characterize metal-organic frameworks and investigate their interaction with guest molecules. Chem Rev 121:1286–1424. https://doi.org/10.1021/acs.chemrev.0c00487

Hanahan D, Robert A W (2017) Biological Hallmarks of cancer. Holland-Frei cancer Med 1–10. https://doi.org/10.1002/9781119000822.hfcm002

Harrison S, Judd J, Chin S, Ragin C (2022) Disparities in lung cancer treatment. Curr Oncol Rep 24:241–248. https://doi.org/10.1007/s11912-022-01193-4

Huang W-C, Chen S-H, Chiang W-H et al (2016) Tumor microenvironment-responsive nanoparticle delivery of chemotherapy for enhanced selective cellular uptake and transportation within tumor. Biomacromolecules 17:3883–3892. https://doi.org/10.1021/acs.biomac.6b00956

Ibrahim WN, Rosli LMBMR, Doolaanea AA (2020) Formulation, Cellular uptake and cytotoxicity of thymoquinone-loaded PLGA nanoparticles in malignant melanoma cancer cells. Int J Nanomedicine 15:8059–8074. https://doi.org/10.2147/IJN.S269340

Kiruthiga C, Balan DJ, Jafni S, Anandan DP, Devi KP (2024) Phytol and (−)-α-bisabolol Synergistically trigger intrinsic apoptosis through redox and Ca2+ imbalance in non-small cell lung cancer. Biocatal Agric Biotechnol 103005. https://doi.org/10.1016/j.bcab.2023.103005

Komiya T, Kyohkon M, Ohwaki S et al (1999) Phytol induces programmed cell death in human lymphoid leukemia Molt 4B cells. Int J Mol Med 4:377–380. https://doi.org/10.3892/ijmm.4.4.377

Lammer E, Carr GJ, Wendler K et al (2009) Is the fish embryo toxicity test (FET) with the zebrafish (Danio rerio) a potential alternative for the fish acute toxicity test? Comp Biochem Physiol Part C Toxicol Pharmacol 149:196–209. https://doi.org/10.1016/j.cbpc.2008.11.006

Lee JH, Yeo Y (2016) Controlled drug release from pharmaceutical nanocarriers Jinhyun. Chem Eng Sci 24:75–84

Makadia HK, Siegel SJ (2011) Poly lactic-co-glycolic acid (PLGA) as biodegradable controlled drug delivery carrier. Polymers (Basel) 3:1377–1397. https://doi.org/10.3390/polym3031377

Marongiu L, Donini M, Bovi M et al (2014) The inclusion into PLGA nanoparticles enables α-bisabolol to efficiently inhibit the human dendritic cell pro-inflammatory activity. J Nanoparticle Res 16:2554. https://doi.org/10.1007/s11051-014-2554-4

Mathew A, Fukuda T, Nagaoka Y et al (2012) Curcumin loaded-PLGA nanoparticles conjugated with Tet-1 peptide for potential use in Alzheimer's disease. PLoS One 7:e32616. https://doi.org/10.1371/journal.pone.0032616

Murata Y, Kokuryo T, Yokoyama Y et al (2017) The anticancer effects of novel α-bisabolol derivatives against pancreatic cancer. Anticancer Res. 37:589–598

Norouzi M, Hardy P (2021) Clinical applications of nanomedicines in lung cancer treatment. Acta Biomater 121:134–142. https://doi.org/10.1016/j.actbio.2020.12.009

Patra JK, Das G, Fraceto LF et al (2018) Nano based drug delivery systems: recent developments and future prospects. J Nanobiotechnology 16:71. https://doi.org/10.1186/s12951-018-0392-8

Picquart M, Lefèvre T (2003) Raman and Fourier transform infrared study of phytol effects on saturated and unsaturated lipid multibilayers. J Raman Spectrosc 34:4–12. https://doi.org/10.1002/jrs.927

Rajavel T, Mohankumar R, Archunan G et al (2017) Beta sitosterol and Daucosterol (phytosterols identified in Grewia tiliaefolia) perturbs cell cycle and induces apoptotic cell death in A549 cells. Sci Rep 7:3418. https://doi.org/10.1038/s41598-017-03511-4

Rajavel T, Packiyaraj P, Suryanarayanan V et al (2018) β-Sitosterol targets Trx/Trx1 reductase to induce apoptosis in A549 cells via ROS mediated mitochondrial dysregulation and p53 activation. Sci Rep 8:2071. https://doi.org/10.1038/s41598-018-20311-6

Ray S, Ghosh RS, Mandal S (2017) Development of bicalutamide-loaded PLGA nanoparticles: preparation, characterization and in-vitro evaluation for the treatment of prostate cancer. Artif Cells, Nanomedicine, Biotechnol 45:944–954. https://doi.org/10.1080/21691401.2016.1196457

Rezvantalab S, Drude NI, Moraveji MK et al (2018) PLGA-based nanoparticles in cancer treatment. Front Pharmacol 9:1260. https://doi.org/10.3389/fphar.2018.01260

Ruirui Z, He J, Xu X et al (2021) PLGA-based drug delivery system for combined therapy of cancer: research progress. Mater Res Express 8:122002. https://doi.org/10.1088/2053-1591/ac3f5e

Sah AK, Suresh PK, Verma VK (2017) PLGA nanoparticles for ocular delivery of loteprednol etabonate: a corneal penetration study. Artif Cells, Nanomedicine, Biotechnol 45:1156–1164. https://doi.org/10.1080/21691401.2016.1203794

Sakthivel R, Malar DS, Devi KP (2018) Phytol shows anti-angiogenic activity and induces apoptosis in A549 cells by depolarizing the mitochondrial membrane potential. Biomed Pharmacother 105:742–752. https://doi.org/10.1016/j.biopha.2018.06.035

Singh V, Tiwari M (2010) Structure-processing-property relationship of poly(glycolic acid) for drug delivery systems 1: synthesis and catalysis. Int J Polym Sci 2010:1–23. https://doi.org/10.1155/2010/652719

Soni S, Gupta H, Kumar N et al (2010) Biodegradable biomaterials. Recent Patents. Biomed Eng 3:30–40. https://doi.org/10.2174/1874764711003010030

Thakor P, Subramanian RB, Thakkar SS et al (2017) Phytol induces ROS mediated apoptosis by induction of caspase 9 and 3 through activation of TRAIL, FAS and TNF receptors and inhibits tumor

progression factor Glucose 6 phosphate dehydrogenase in lung carcinoma cell line (A549). Biomed Pharmacother 92:491–500. https://doi.org/10.1016/j.biopha.2017.05.066

Varani M, Galli F, Capriotti G et al (2020) Theranostic designed near-infrared fluorescent poly (lactic-co-glycolic acid) nanoparticles and preliminary studies with functionalized VEGF-nanoparticles. J Clin Med 9:1750. https://doi.org/10.3390/jcm9061750

Wang Y, Li P, Kong L (2013) Chitosan-modified PLGA nanoparticles with versatile surface for improved drug delivery. AAPS PharmSciTech 14:585–592. https://doi.org/10.1208/s12249-013-9943-3

Wei W, Zhang X, Chen X et al (2016) Smart surface coating of drug nanoparticles with cross-linkable polyethylene glycol for bioresponsive and highly efficient drug delivery. Nanoscale 8:8118–8125. https://doi.org/10.1039/C5NR09167E

Wen Y-H, Lee T-Y, Fu P-C et al (2017) Multifunctional polymer nanoparticles for dual drug release and cancer cell targeting. Polymers (Basel) 9:213. https://doi.org/10.3390/polym9060213

Weng J, Tong HHY, Chow SF (2020) In vitro release study of the polymeric drug nanoparticles: development and validation of a novel method. Pharmaceutics 12:732. https://doi.org/10.3390/pharmaceutics12080732

Wu S, Peng L, Sang H et al (2018) Anticancer effects of α-Bisabolol in human non-small cell lung carcinoma cells are mediated via apoptosis induction, cell cycle arrest, inhibition of cell migration and invasion and upregulation of P13K/AKT signalling pathway. J BUON 23:1407–1412

Xie B, Liu T, Chen S et al (2021) Combination of DNA demethylation and chemotherapy to trigger cell pyroptosis for inhalation treatment of lung cancer. Nanoscale 13:18608–18615. https://doi.org/10.1039/D1NR05001J

Yao Y, Zang Y, Qu J et al (2019) The toxicity of metallic nanoparticles on liver: the subcellular damages, mechanisms, and outcomes. Int J Nanomedicine 14:8787–8804